Bias of Earthquake Depths Towards Layer Interfaces

Bill Menke, October 25, 2026

Part 1. Travel Times. We consider an Earth model consisting of a low-velocity layer over a half space. All events and stations are confined to the $(x, y = 0, z)$ plane. First arrival travel times for the P_g, P_n and P_2 rays are considered (Fig. 1).

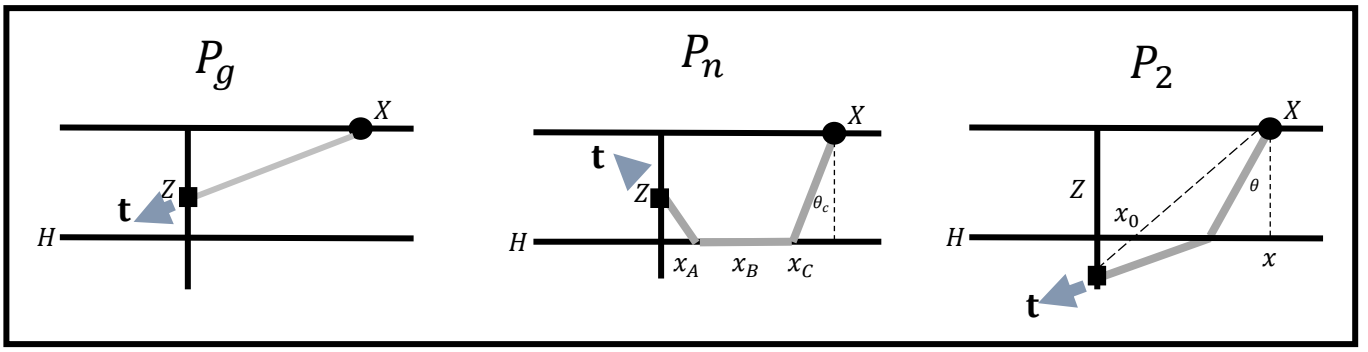


Fig. 1. The model is a layer of thickness H and slowness s_1 over a half-space of slowness $s_2 < s_1$. Three ray paths (lines) are considered that connect the event (square) at $(0, Z)$ with the station (circle) at $(X, 0)$ and are denoted P_g, P_n and P_n. The tangent vector **t** (arrow) is at the event in the direction of increasing ray length.

The travel time and tangent along the P_g ray is:

$$T = [X^2 + Z^2]^{1/2} \qquad \mathbf{t} \propto \begin{bmatrix} -X \\ Z \end{bmatrix}$$

The travel time and tangent along the P_n ray is:

$$\sin(\theta_c) = s_2/s_1$$

$$x_A = (H - Z)\tan(\theta_c) \qquad T_A = s_1(x_A^2 + (H - Z)^2)^{1/2}$$

$$x_B = X - (x_A + x_C) \qquad T_B = s_2 x_B$$

$$x_C = H\tan(\theta_c) \qquad T_C = s_1(x_C^2 + H^2)^{1/2}$$

$$T = T_A + T_B + T_C \qquad \mathbf{t} \propto \begin{bmatrix} -x_A \\ -(H - Z) \end{bmatrix}$$

This ray path exists only when x_B>0.

In order to find the travel time and tangent along the P_2 ray, the position (x, H) that satisfies Snell's law muster be determined. We use Fermat's principle, which state that the travel time is an extremum at this point. For a arbitrary point x:

$$T = s_1\left((X-x)^2 + H^2\right)^{½} + s_2(x^2 + (Z-H)^2)^{½}$$

$$T' \equiv \frac{dT}{dx} = -s_1(X-x)\left((X-x)^2 + H^2\right)^{-½} + s_2 x(x^2 + (Z-H)^2)^{-½}$$

$$T'' \equiv \frac{d^2T}{dx^2} = s_1\left((X-x)^2 + H^2\right)^{-½} + s_2(x^2 + (Z-H)^2)^{-½}$$
$$-s_1(X-x)^2\left((X-x)^2 + H^2\right)^{-3/2} - s_2 x^2(x^2 + (Z-H)^2)^{-3/2}$$

Newtoinian iteration $x_{n+1} = x_n - T'/T''$ is then used to find the extremum, with the starting guess $x_0 = X(Z-H)/H$. The tangent vector is:

$$\mathbf{t} \propto \begin{bmatrix} -x \\ -(Z-H) \end{bmatrix}$$

As the problem has translational symmetry, events at $x \neq 0$ are handled by a coordinate shift.

Part 2. Error surfaces. We consider and Earth model with $s_1^{-1} = 5$ km/s, $s_2^{-1} = 6.5$ km/s and $H = 5$ km. Travel times of an event at (x^{eve}, z^{eve}) are observed at stations at $\{x_i^{sta}, i = 1 \cdots N\}$. In the examples shown here, $N = 8$ and the $-1.2 \leq x_i^{sta} < 5.1$.

We examine the L_2 travel time error surface $E(x, z)$ for a single event observed on the stations, for two case, $z < H$ and $z > H$ (Fig. 2).

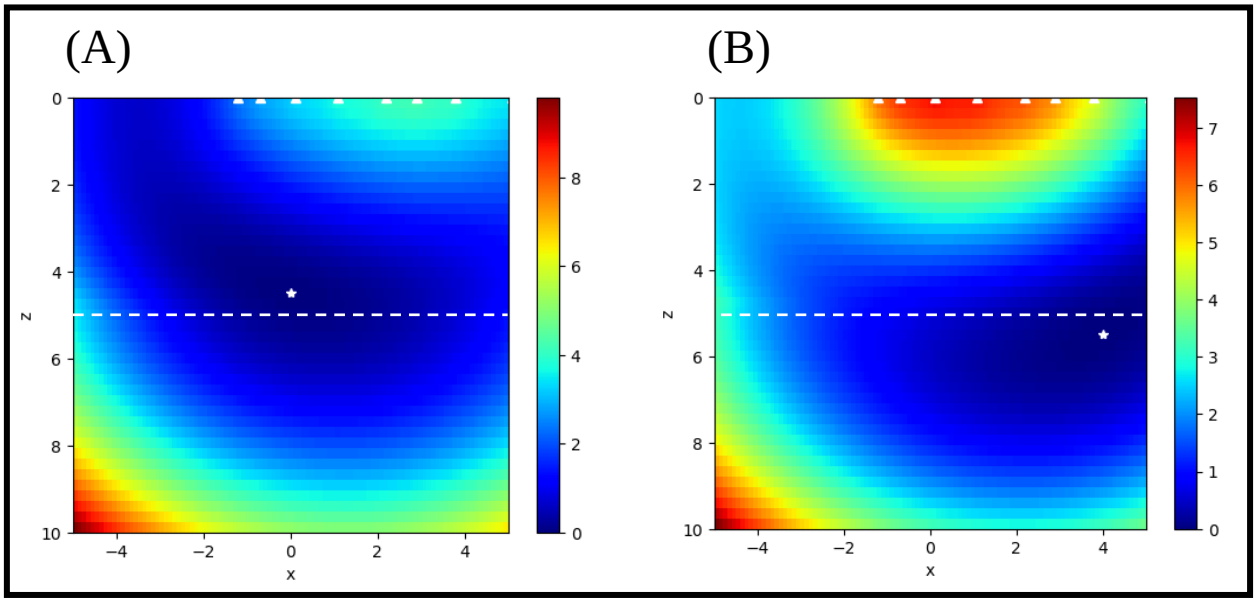


Fig. 2. Error surface $E(x, z)$ (colors) for a single event (star) observed on an array of stations (triangles). (A) Event within the low-velocity layer (dashed line). (B) Event below the layer.

In both cases, a well-defined error minimum is co-located with the event. This results gives confidence that the event can be well-located.

Part 3. Geiger's method. Geiger's method is an iterative least-squares eartyhquake location procedure with three model parameters, $\mathbf{m} = [x^{eve}, z^{eve}, \tau\,]^T$, where τ is origin time. The iterative procedure updates an initial guess for the model parameters using the recursion $\mathbf{m}^{(n+1)} = \mathbf{m}^{(n)} + \Delta\mathbf{m}$, where $\Delta\mathbf{m}$ is the least squares solution to $\mathbf{G}\Delta\mathbf{m} = \Delta\mathbf{d}$ and $\Delta d_i = T^{obs}\left(x_i^{sta}\right) - T^{pre}\left(x_i^{sta}, \mathbf{m}^n\right)$. Here, T^{obs} and T^{pre} are the observed and predicted arrival times, respectively. The $N \times 3$ matrix $\mathbf{G}$ is has columns $G_{i,1} = t_x^{(i)}$, $G_{i,2} = t_z^{(i)}$ and $G_{i,3} = 1$. Although the true origin time will always be zero in our examples, its least squares estimate will *not* be zero. Furthermore, the estimated event location and estimated event location will be shown to trade off in important ways. In our simulations, the starting location is the true location, plus a 0.1 km random perturbation

Part 4. Depth Bias. We perform test in which groups of 50 events are placed on each node of a sparse (x, z) grid, travel times are computed from them to an array of stations and each station is located individually by Geiger's method.

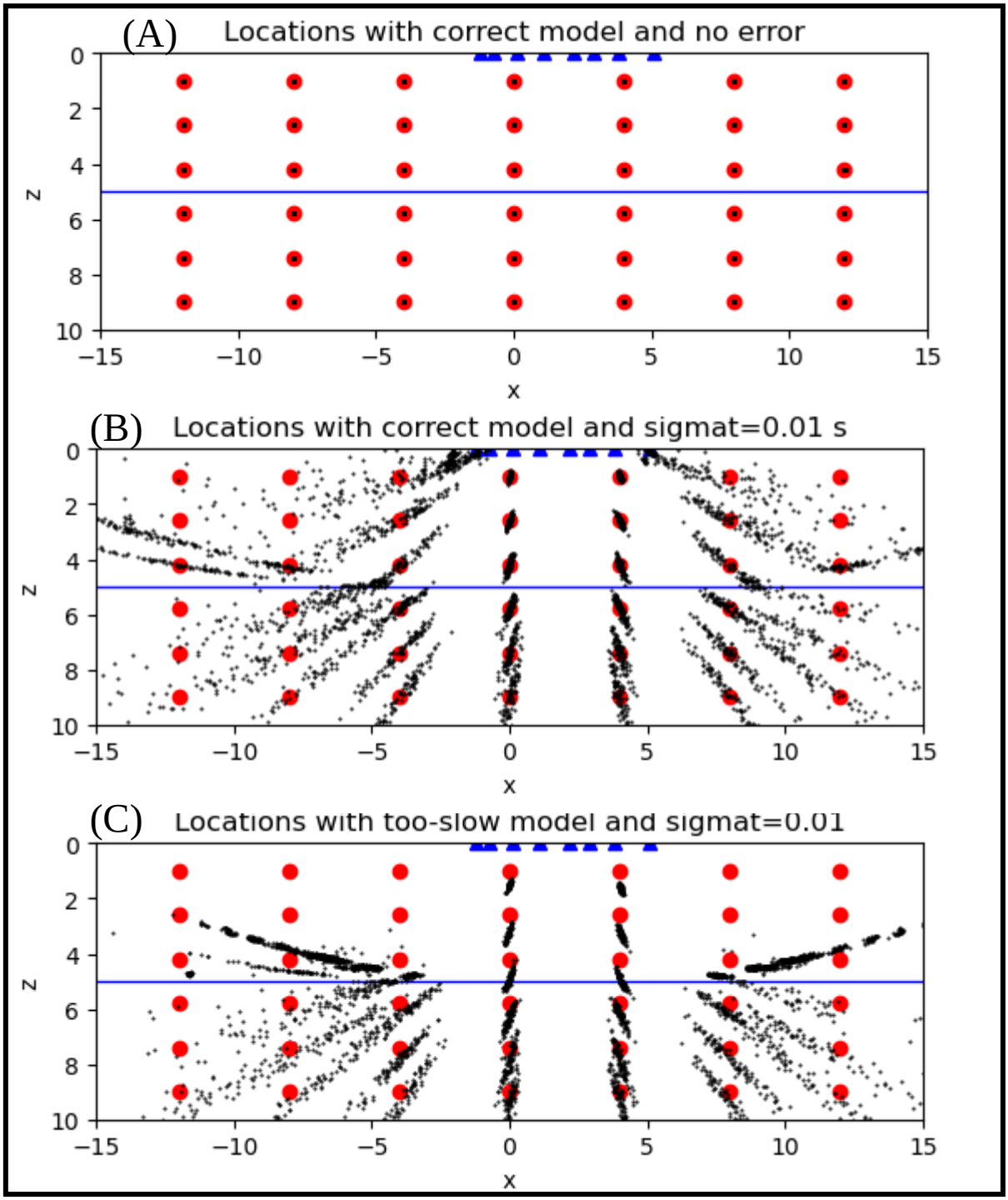


Fig. 3. Event location experiment, showing grid points (red dots), earthquake locations (black dots), stations (triangles) and layer boundary (blue line). See text for further discussion.

When no observation noise is present, the predicted event locations (Fig. 3A, black dots) are all close to their true locations (red dots). Further experiments (not shown) demonstrate that this good correspondence requires that the initial location be within about 2 km of the true location. Events outside the array footprint are particularly sensitive to the initial location.

We then perturb arrival times with Normally distributed random noise with zero mean and variance of $\sigma_t^2 = (0.01\ s)^2$ (Fig. 3B). Groups of events corresponding to an individual grid point now exhibit significant scatter, especially in depth. The scatter tends to be small (< 1 km) within the array footprint, and increases to > 5 km for events outside the array. In most cases, the scatter tends to be centered around the grid points.

When the layer velocity used in Geiger's method is incorrect (say $s_1^{-1} =$ 4.5 km/s (lower than the true value of 5) (Fig. 3C), the scatter of the events is systematical biased away from the grid points. As we show below, this effect is involves origin time trading off with depth.

Part 5. Explanation of Depth Bias. We start by considering an event at a depth of 4 km in a model with $s_1^{-1} = 5$ km/s. It's travel time curve (Fig. 4A, black curve) has lower curvature than does the prediction of a model with $s_1^{-1} =$ 4 km/s . The overall root mean squared arrival time error is 0.11 s. However, a deeper event has a travel time curve less curvature – but also one that is delayed. The error can be reduced to 0.03 s by making it deeper, adjusting the origin time to compensate for the overall arrival time shift (Fig. 4B). However, if the event is near a layer boundary, moving it below the boundary typically increases the error (Fig. 4C) (to 0.06 s in the example).

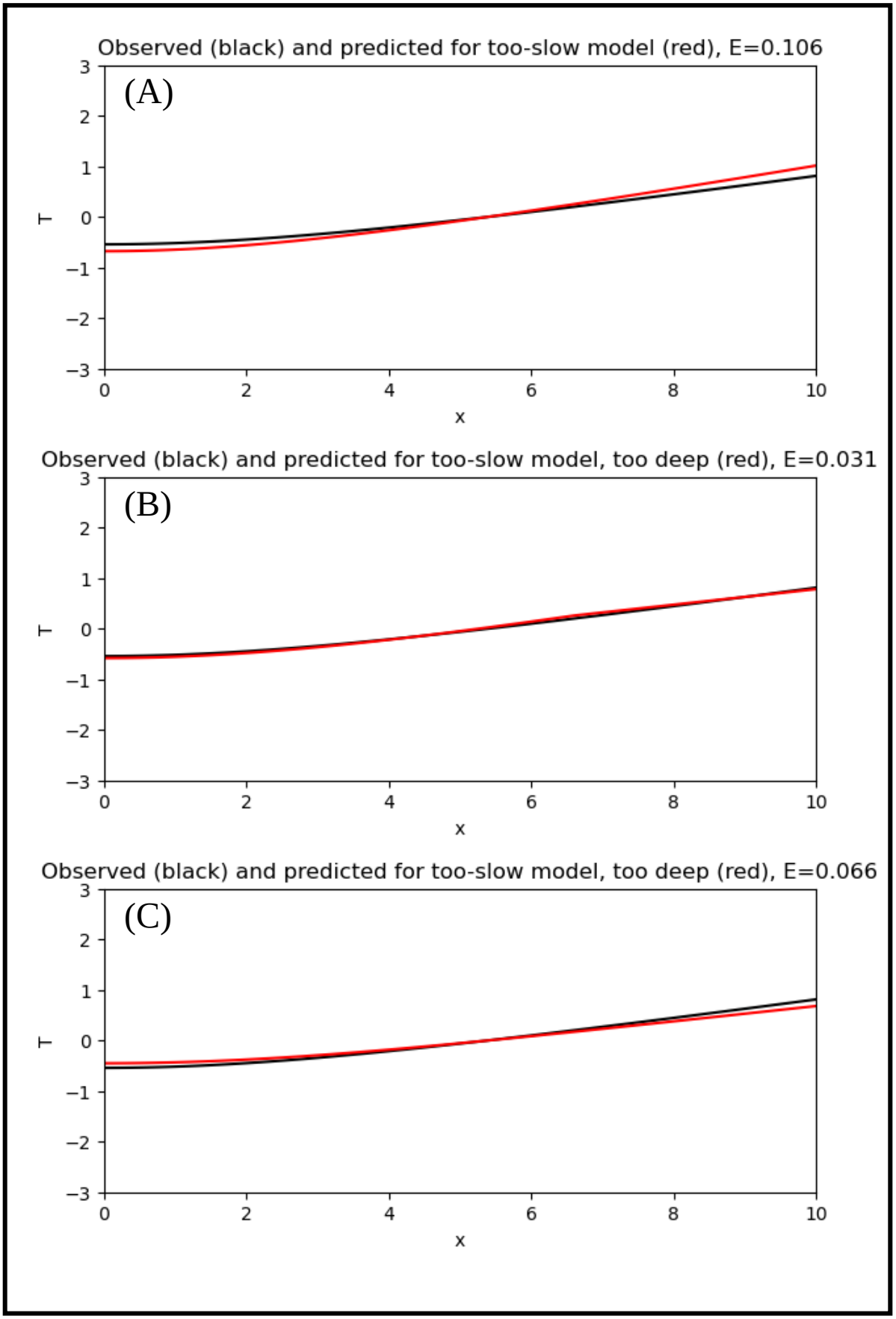


Fig. 4. Observed (black) and predicted arrival time curves, See text for further explanation,

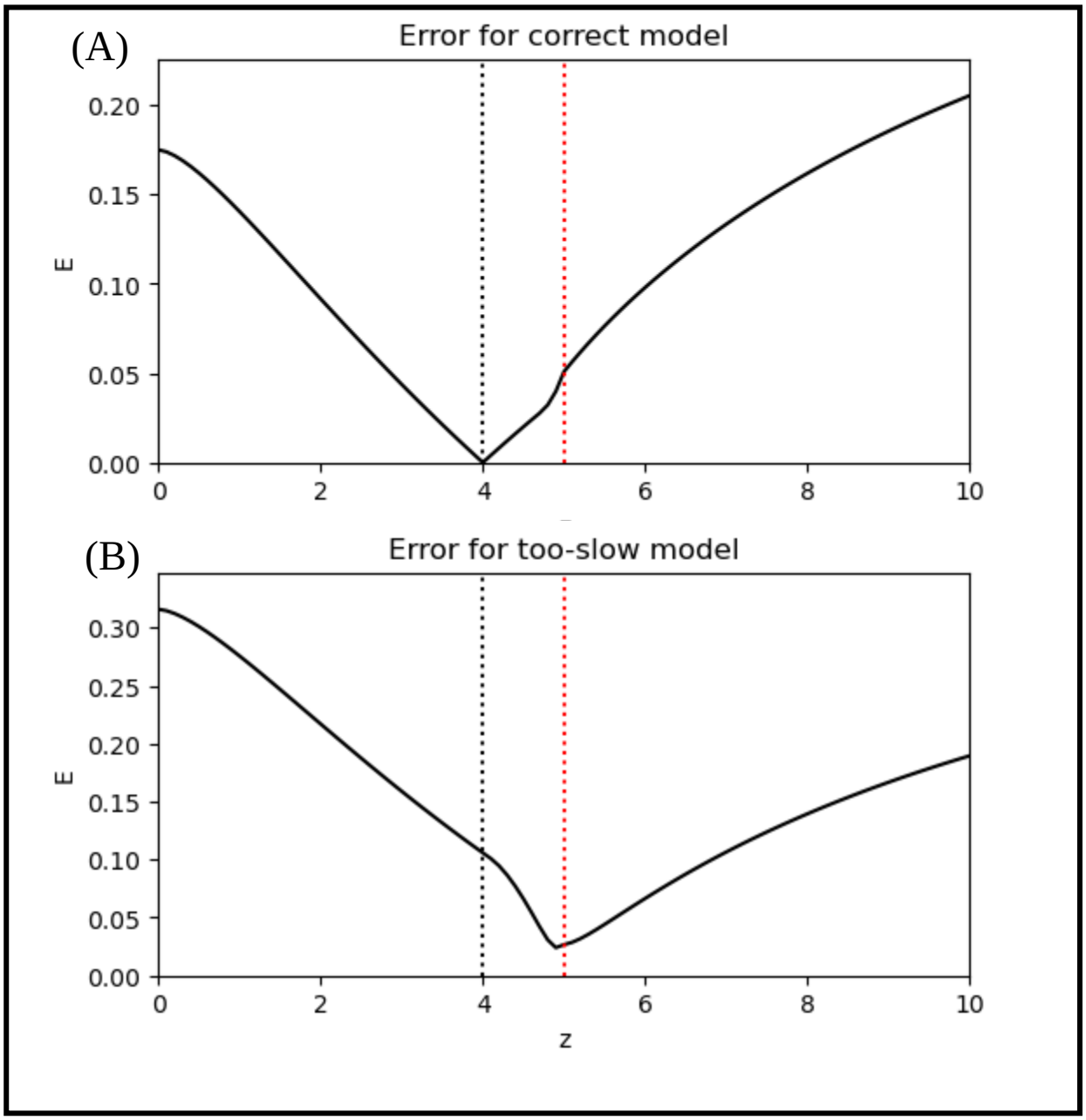


Fig. 5. Effect of incorrect depth on the root mean squared travel time error *solid curve). The earthquake depth (dotted black line) and layer thickness (dotted red curve are also shown. (A) Error for a model with the correct layer velocity of $s_1^{-1} = 5$ km/s. (B) Error for a model with the incorrect layer velocity of $s_1^{-1} = 4$ km/s.

Numerical experiment (Fig 5) demonstrates that the minimum error occurs near the true depth when correct model is used, but can move to the layer interface when the model is too slow.

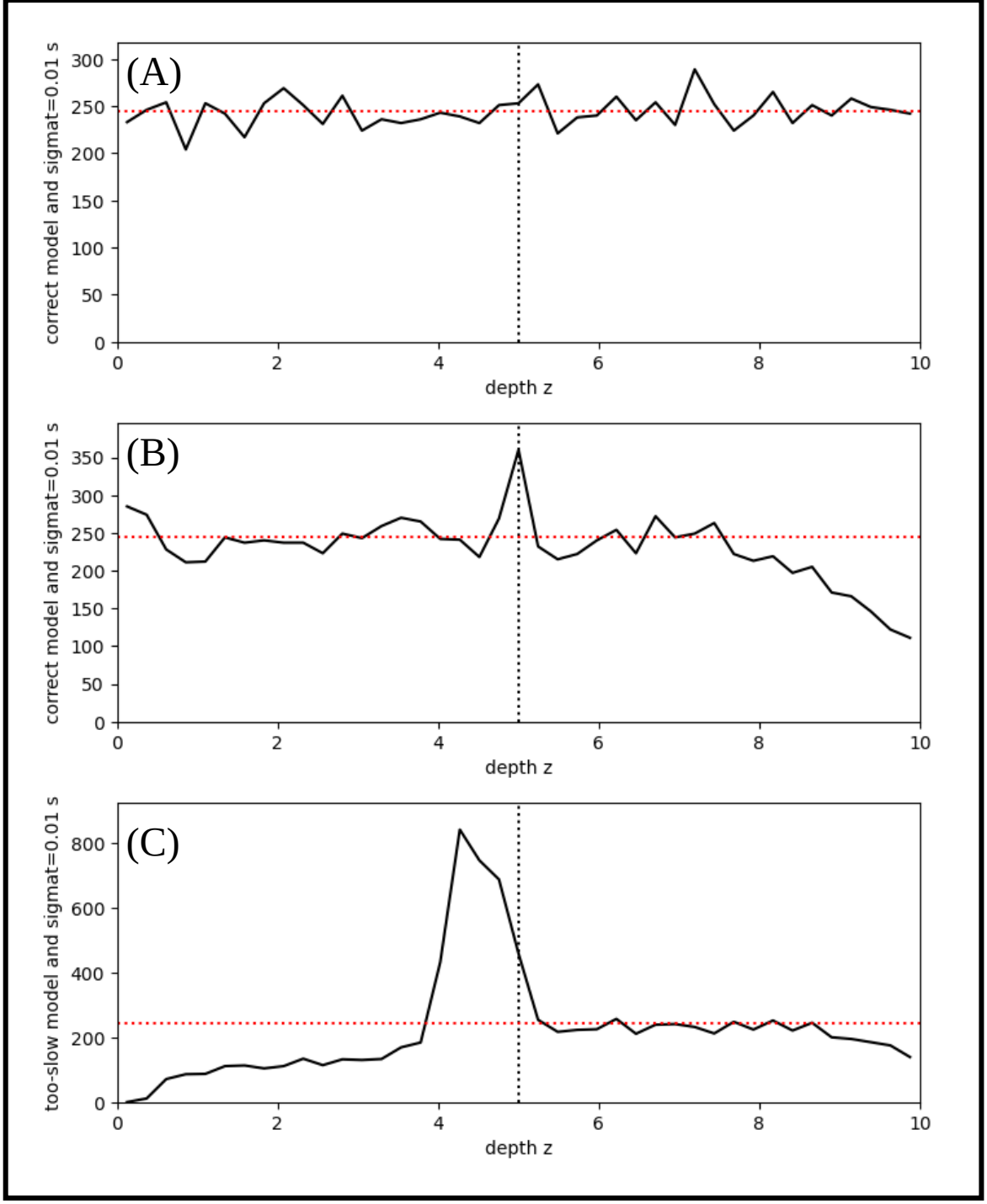


Fig. 6. Histograms of estimated event depth, for uniformly distributed true depths. The events also have uniformly distributed horizontal positions in the $(-10,10)$ km interval. (A) No arrival time noise and correct Earth model. (B) Small arrival time noise with $\sigma_t^2 = (0.01\ s)^2$ and correct Earth model. (C) Small arrival time noise with $\sigma_t^2 = (0.01\ s)^2$ and incorrect Earth model with $s_1^{-1} = 4.5$ km/s.

Part 6. Histograms and Scatter Plots of Depth. We investigate this effect by creating a uniformly distributed ensemble of events in the horizontal interval of $(-10,10)$ and the vertical interval of $(0,10)$. Histograms of depth are then used to evaluate (by eye) whether any depths are favored. The histogram is approximately uniform (that is, no depth is favored) when the travel time data contain no noise and the events are located using the correct Earth model (Fig 6A). The depth $z^{est} \approx H$ is favored when the travel time is perturbed with a low level of noise ($\sigma_t^2 = (0.01\ s)^2$) and the correct model is used (Fig. 6B). The depth range $z^{true} < z^{est} < H$ is strongly favored when the travel time is perturbed with a low level of noise ($\sigma_t^2 = (0.01\ s)^2$) and an incorrect "slow" model is used ($s_1^{-1} =$ 4.5 km/s). A pairwise scatter plots of depth illustrates this effect (Fig. 7).

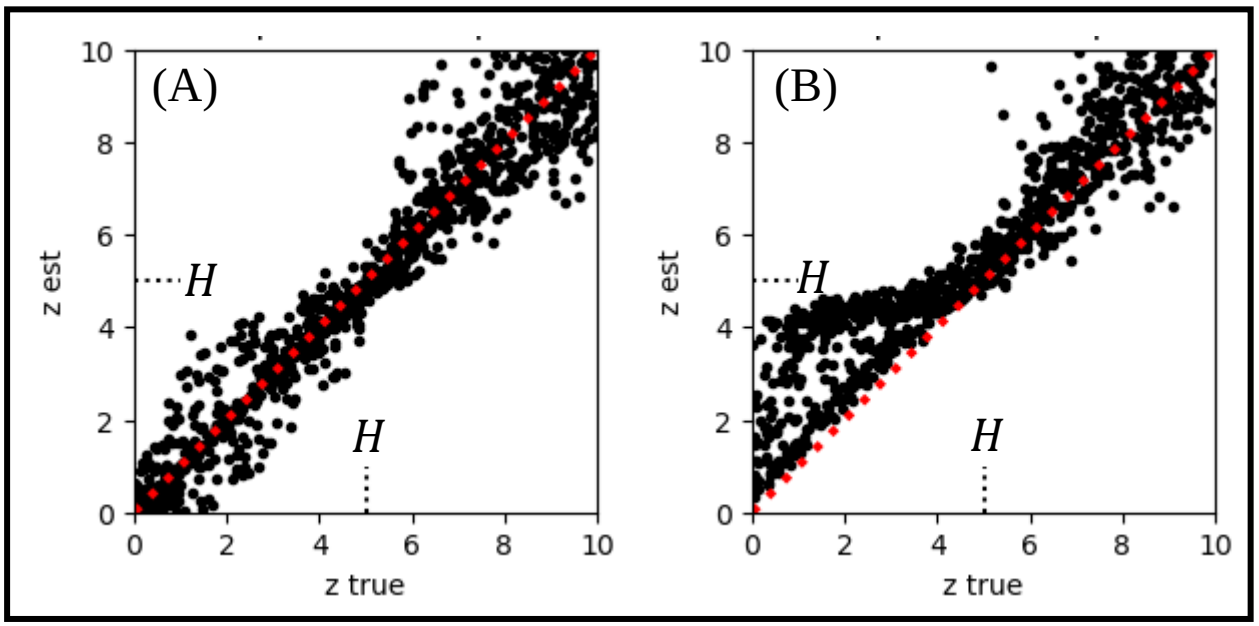


Fig. 7. Scatter plots of true depth z^{true}, drawn from a uniform distribution and estimated depth z^{est}, based on noisy P-wave data ($\sigma_t^2 = (0.01\ s)^2$) , with 1:1 line (red) and layer thickness H (black dotted lines) also shown. (A) Correct model ($s_1^{-1} = 5.0$ km/s). (B) Incorrect model ($s_1^{-1} =$ 4.5 km/s). T

The curvature mechanism that I have identified explains why a incorrect Earth model causes a large peak in the histogram, and a strong clustering of events, at $z = H$ (Figs. 6C and 7B). It does not explain why arrival time noise causes a smaller peak (Fig. 6B). One possibility is that the noise occasionally increases the overall curvature of the arrival time curve, which then causes the least squares algorithm to attempt to deepen the event. Clustering will occur when the deepening crosses a layer interface, because the sudden change in slowness can cause the arrival time error to grow.

Part 8. Effect of Adding S-wave Data. Many earthquake location events include S wave travel times. They are important because the S-P times provide information about the depth of the event that is independent of that provided by the curvature of the P arrival time curve. However, because the S wave is a secondary arrival, the variance of it arrival times is usually much worse than that of the P wave. We modify our Geiger's method software to use both P and S travel times, with a fixed slowness ration $s^S = 1.8s^P$. Least squares errors are weighted by an assumed accuracy. We use $\sigma_t^S = 10\sigma_t^P = 0.1$ s.

When the correct model is used, the overall amount of scatter is reduced compared to the P-wave only case, and no boas is detected (Fig. 8A). However, when the velocity model is incorrect, the events are still biased to a depth close to, but somewhat shallower than, the layer interface H (though less so than for P waves, alone; compare Fig 6B and 8B).

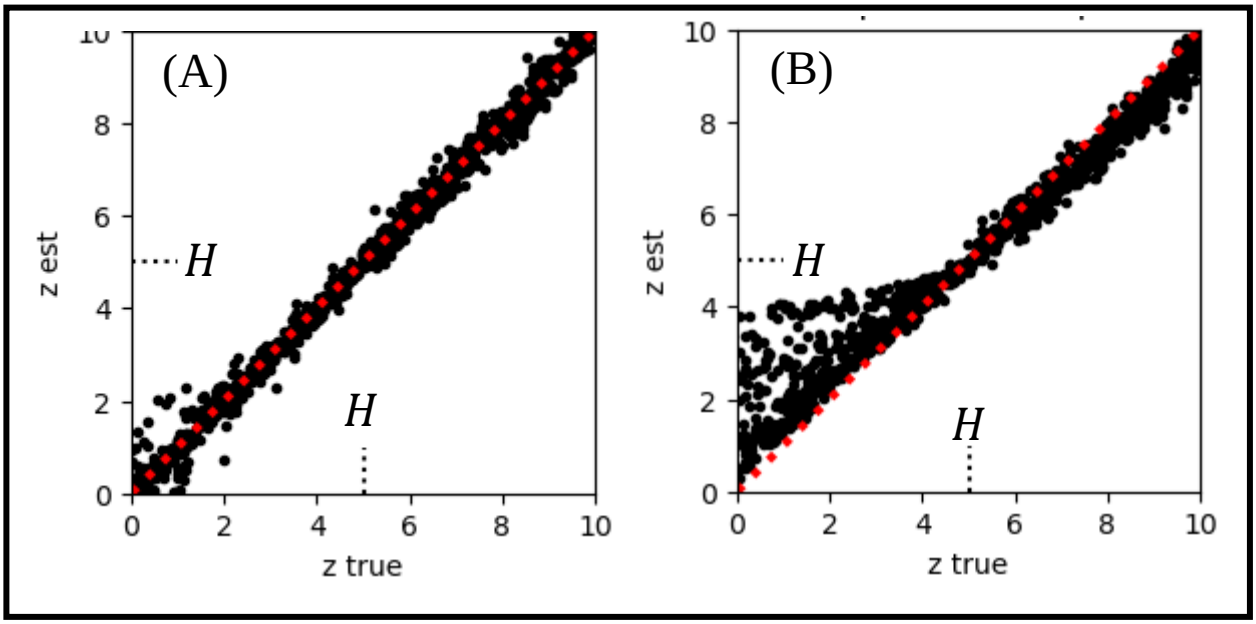


Fig. 8. Scatter plots of true depth z^{true}, drawn from a uniform distribution and estimated depth z^{est}, based on noisy P-wave and S-wave data ($\sigma_t^P = 0.01$ s and $\sigma_t^P = 0.10$ s), with 1:1 line (red) and layer thickness H (black dotted lines) also shown. (A) Correct model ($s_1^{-1} = 5.0$ km/s). (B) Incorrect model ($s_1^{-1} = 4.5$ km/s).